

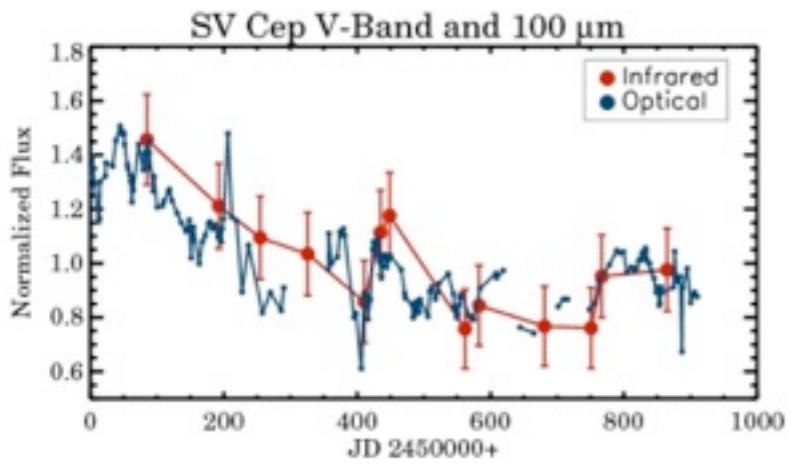
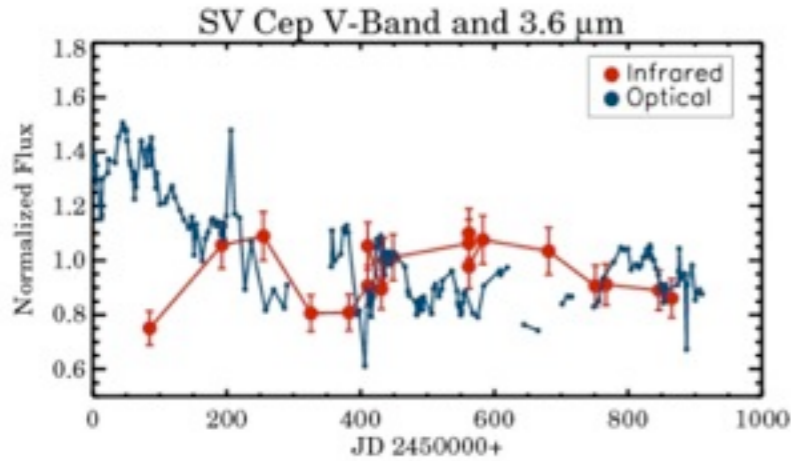
Infrared variability of protoplanetary disks



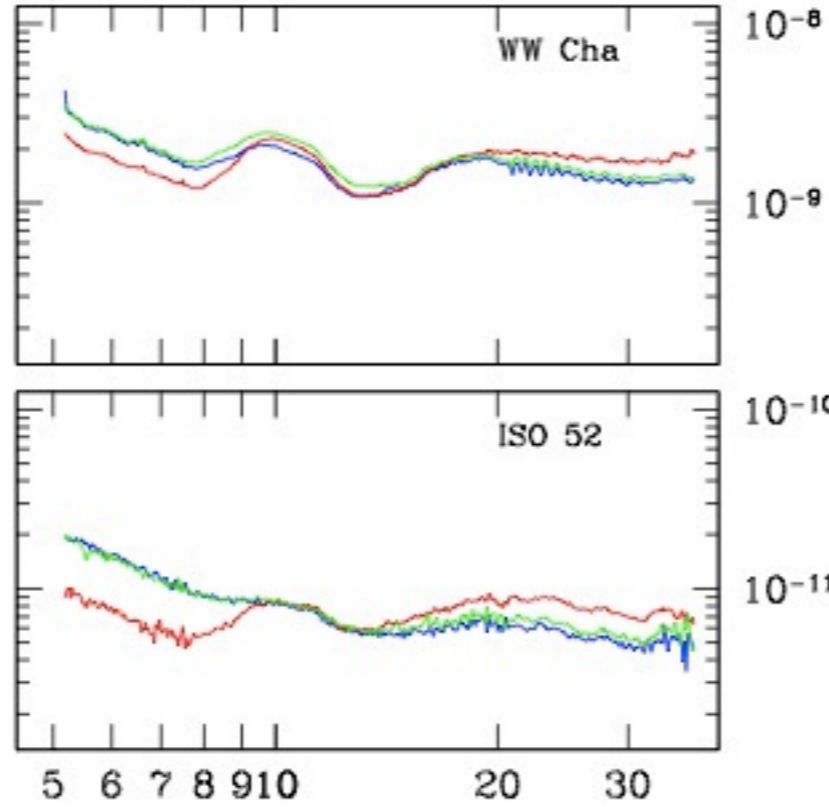
Attila Juhasz¹, Myriam Benisty², Laszlo Mosoni³, Cornelis Dullemond⁴

*Leiden Observatory, Leiden, The Netherlands
Laboratoire d'astrophysique de Grenoble, Grenoble, France
Konkoly Observatory, Budapest, Hungary
Institute for Theoretical Astrophysics, Heidelberg, Germany*

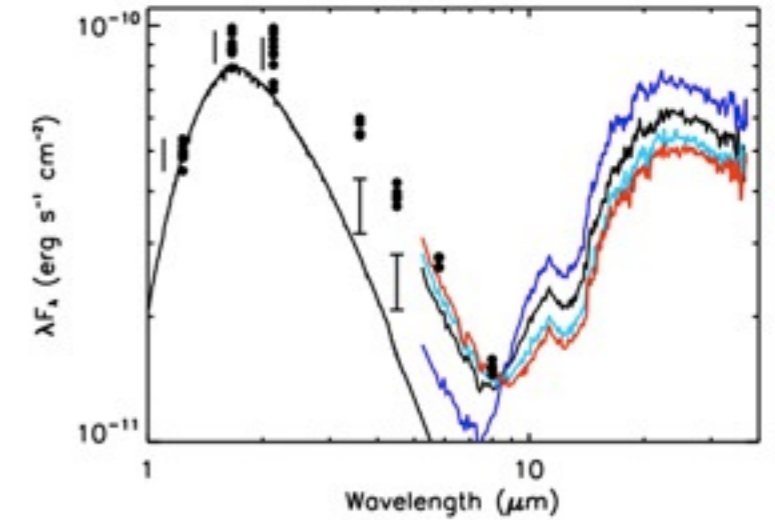
Observed photometric variability



SV Cep, Juhasz et al. 2007



WW Cha, ISO 52, Espaillat et al. 2011

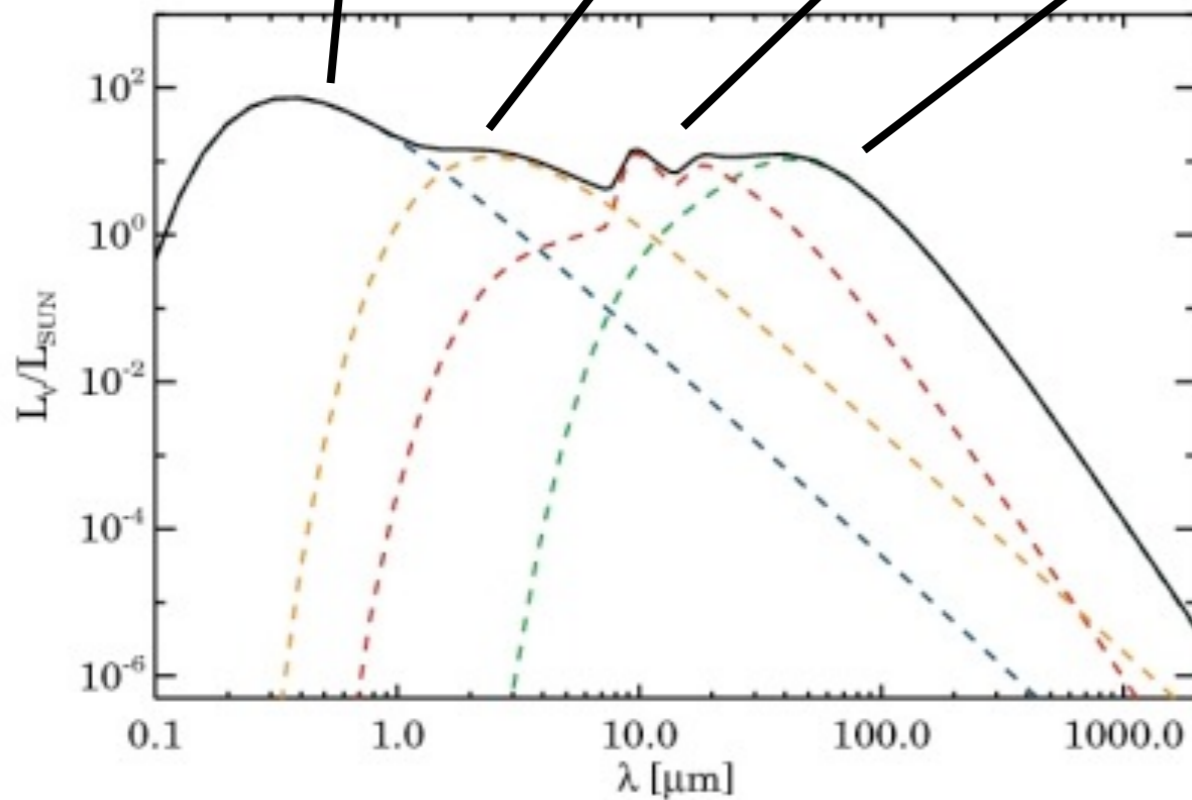
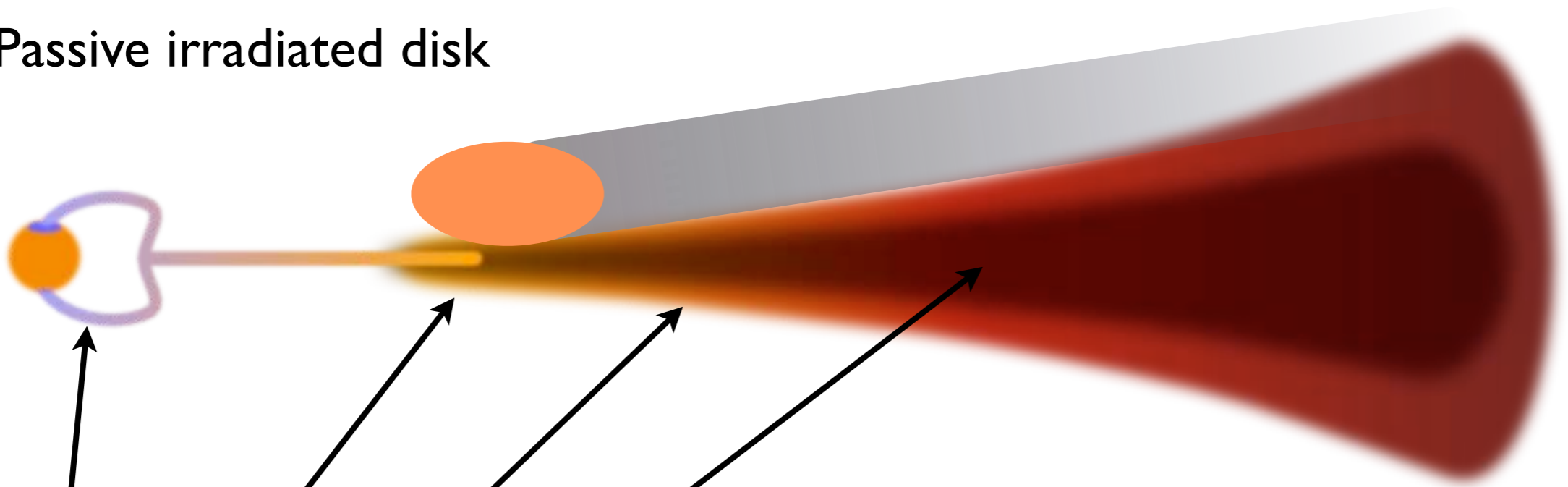


LRL 31, Flaherty et al. 2011

Spitzer warm phase observations (YSOVAR) : a significant fraction of the observed young stars show variability at infrared wavelengths

Source of variability

Passive irradiated disk



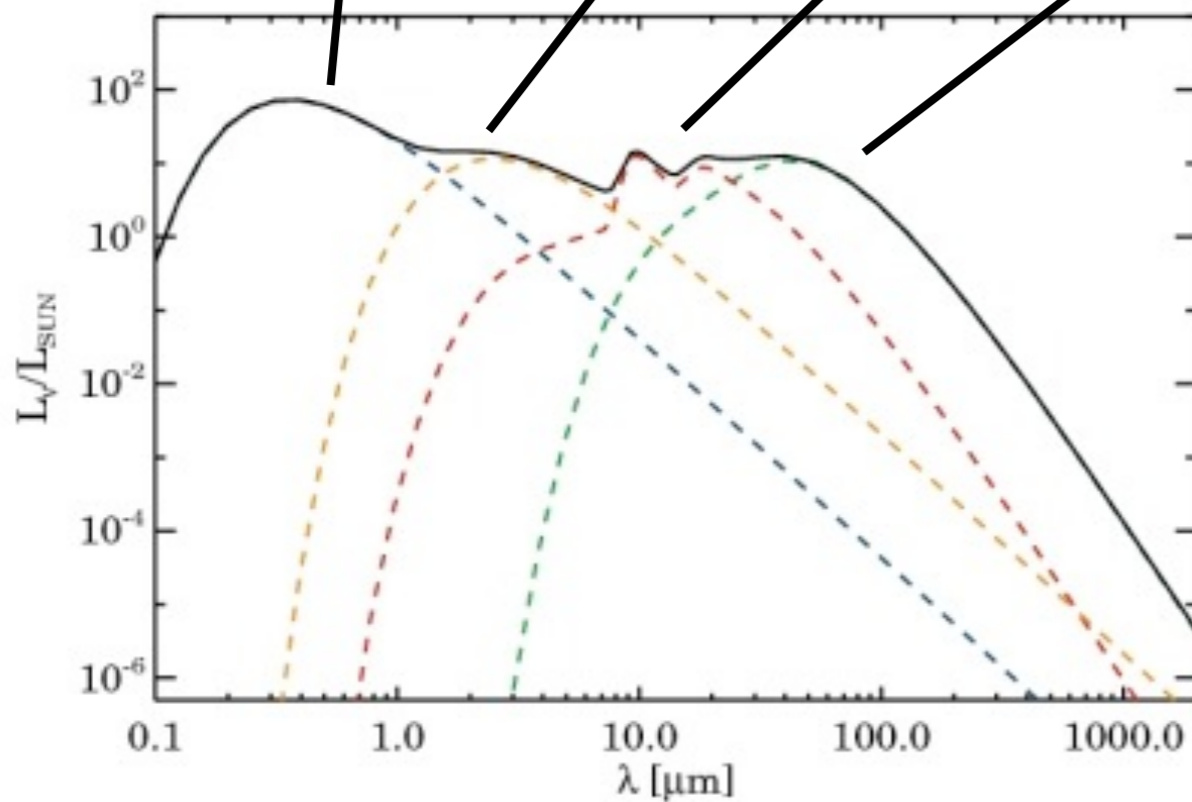
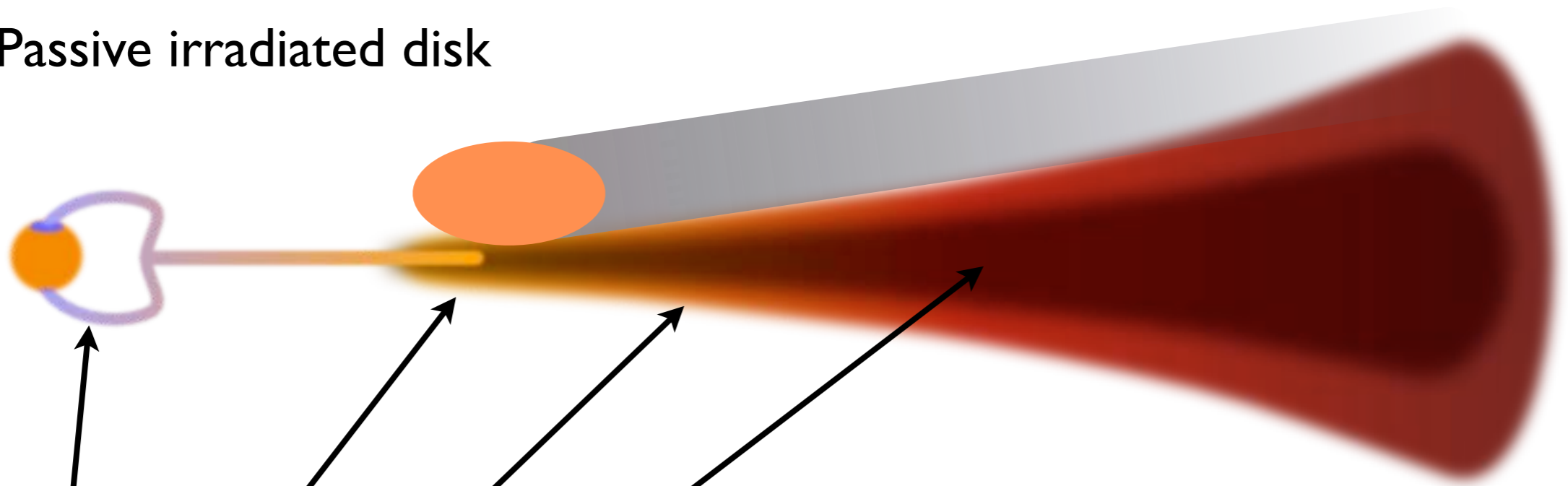
Variability at short wavelenghts (few um)

Short time-scale (several weeks to years)

=>Source of the variability should be located in the inner disk (few AUs at most)

Source of variability

Passive irradiated disk



Proposed scenarios:

- Warped inner disk (e.g. Flaherty et al. 2011)
- Variable disk wind (e.g. Sitko et al. 2008)
- Changes in the scale-height of the inner disk (e.g. Juhasz et al. 2007, Sitko et al. 2008)

Modeling

Take the most frequently invoked models (warp, disk wind, variable inner rim)
use a full 3D RT code (RADMC-3D) to study

- Wavelength dependence of photometric variability
- Signatures of these perturbation in interferometric measurements at NIR/MIR wavelengths

Can we distinguish between these models on the basis of photometric light curve alone?

Would near-infrared interferometry help to separate models?

Or the combination of both?

Modeling

RT code	: RADMC-3D (Dullemond et al., in prep)
Stellar parameters	: $R=2.0R_{\odot}$, $T_{\text{eff}} = 7500\text{K}$
Dust distribution	: $0.1\mu\text{m} - 1\text{mm}$, $n(a)\sim a^{-3.5}$
Opacity	: Weingartner & Draine 2001 (astronomical silicate)
Inner radius	: 0.25AU ($T=1500\text{K}$)
Outer radius	: 200AU
Disk mass	: $0.01M_{\odot}$

Unperturbed disk structure:

$$\rho(r, z, \phi) = \frac{\Sigma(r)}{H_p \sqrt{2\pi}} \exp\left[-\frac{z^2}{2H_p^2}\right]$$

$$\Sigma(r) = \Sigma_0 \left(\frac{r}{r_0}\right)^{-p}$$

Calculate SEDs to see the wavelength dependence of the variability

Calculate images and interferometric quantities

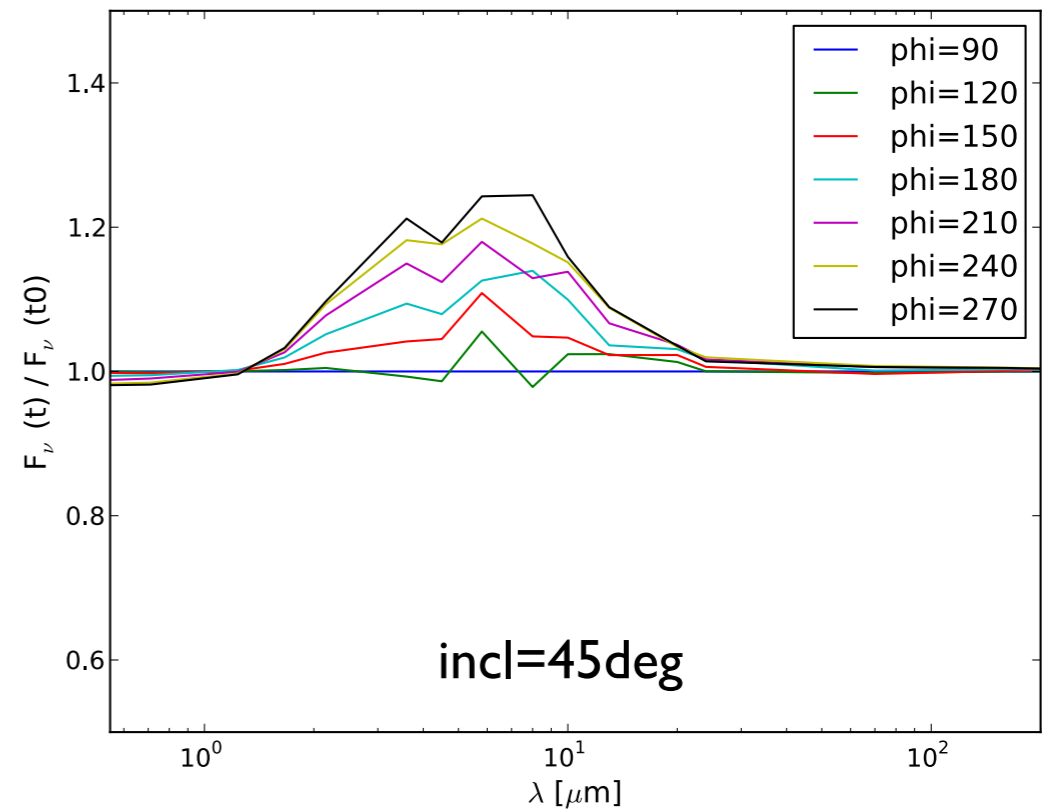
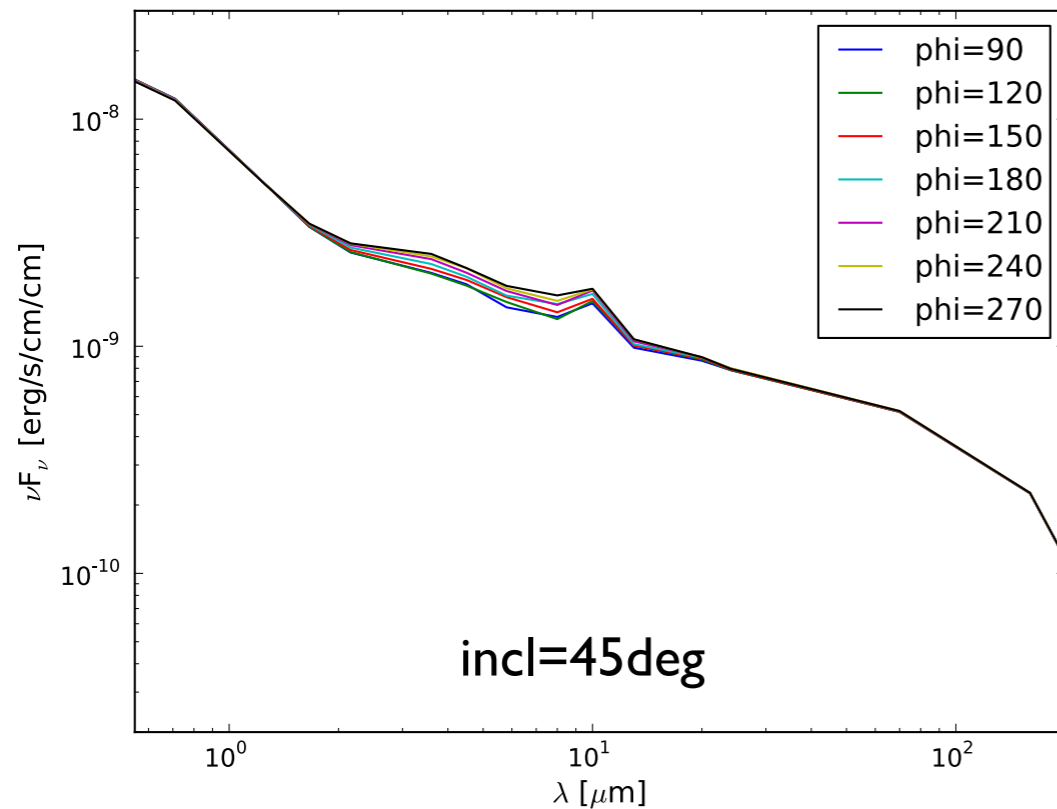
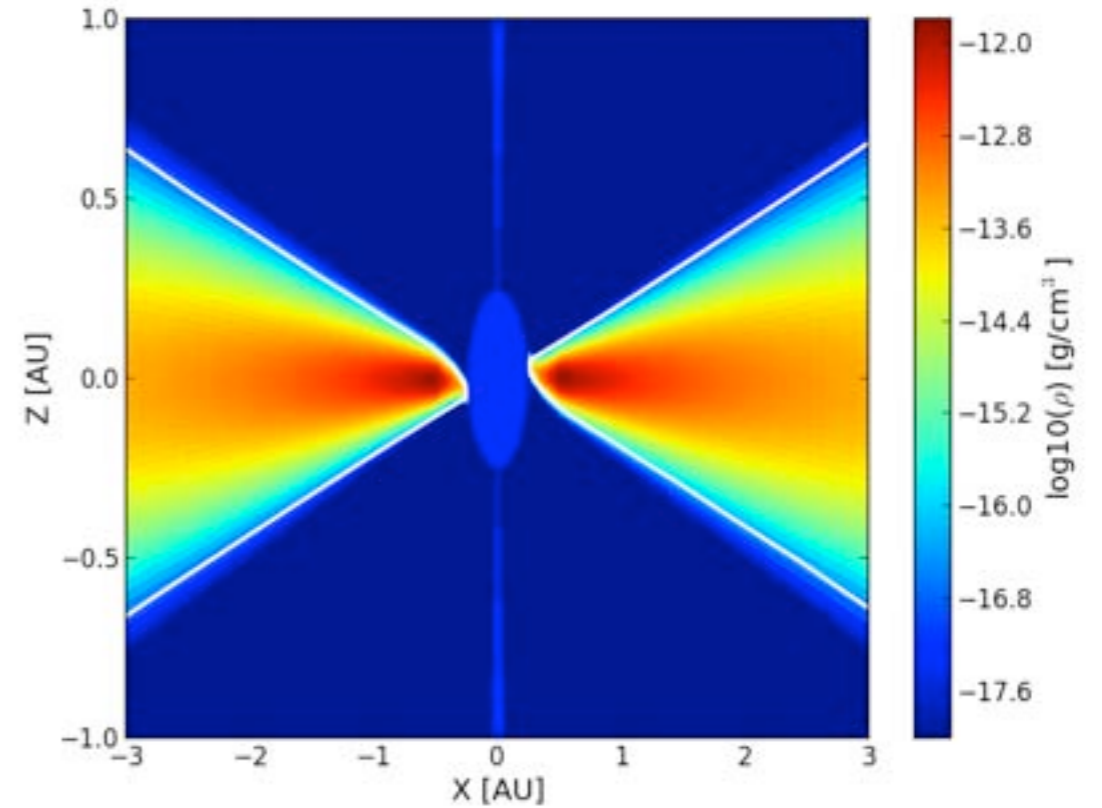
Warped disk

Model:

$$\rho(r, z, \phi) = \frac{\Sigma(r)}{H_p \sqrt{2\pi}} \exp \left[-\frac{(z - z_0(r, \phi))^2}{2H_p^2} \right]$$

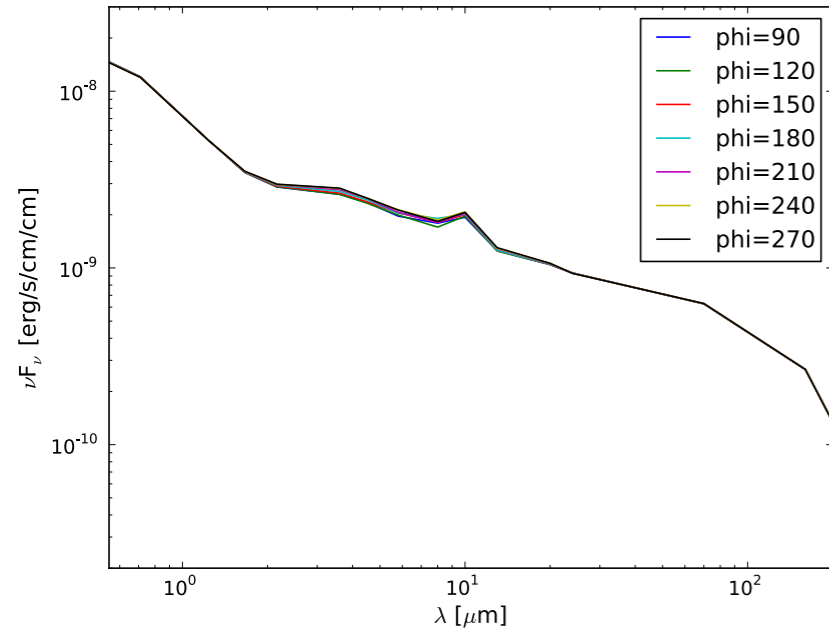
$$z_0(r, \phi) = f \left(\frac{r}{r_{\text{in}}} \right)^{-4} \cos \phi$$

Variability is caused by the rotation/
precession of the warp due to line-
of-sight effects

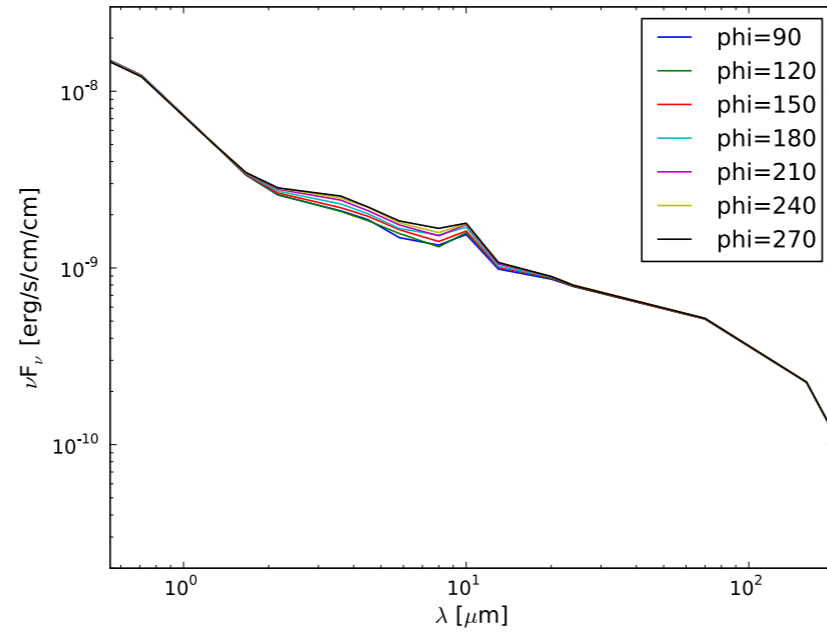


Warped disk

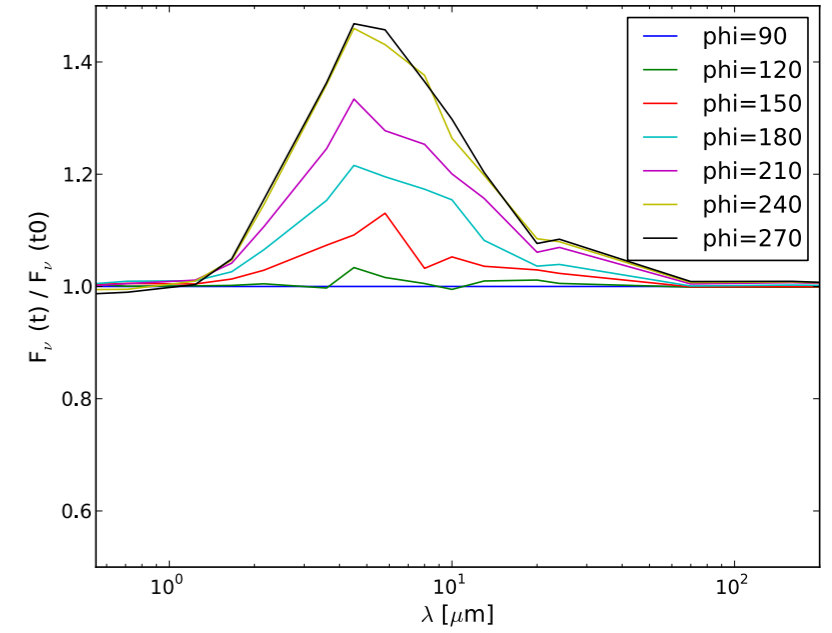
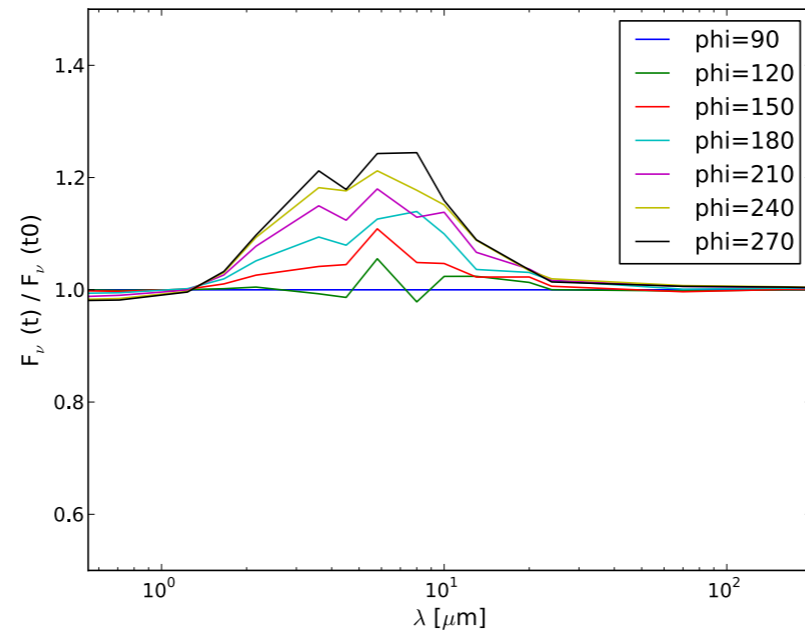
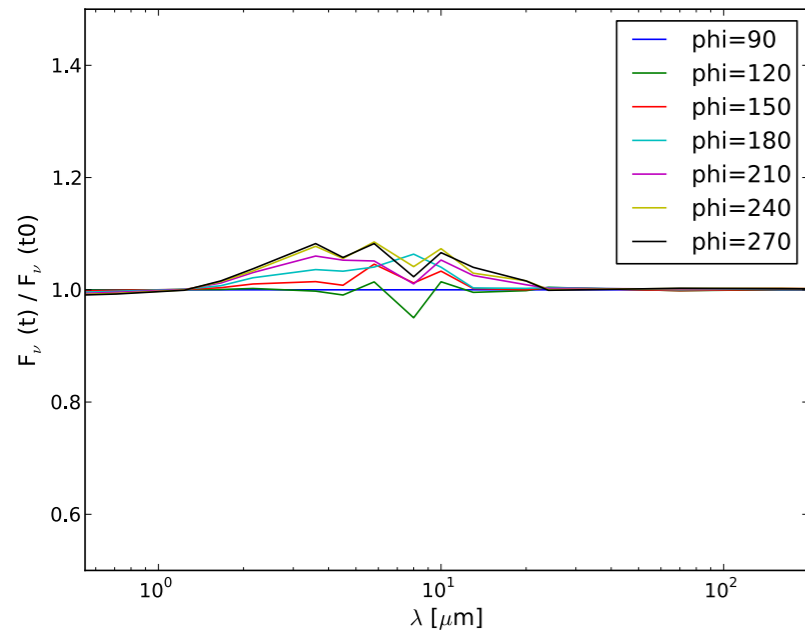
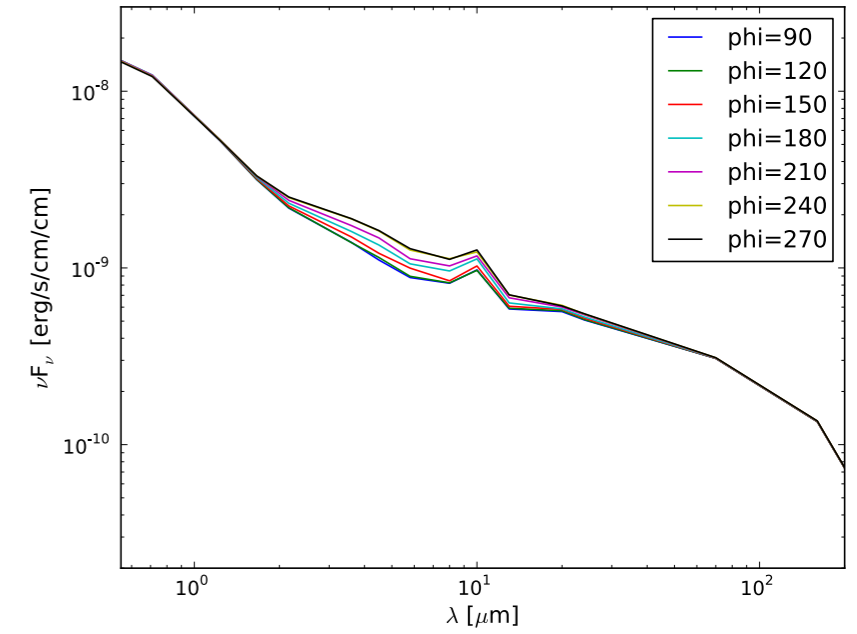
incl=20deg



incl=45deg



incl=70deg



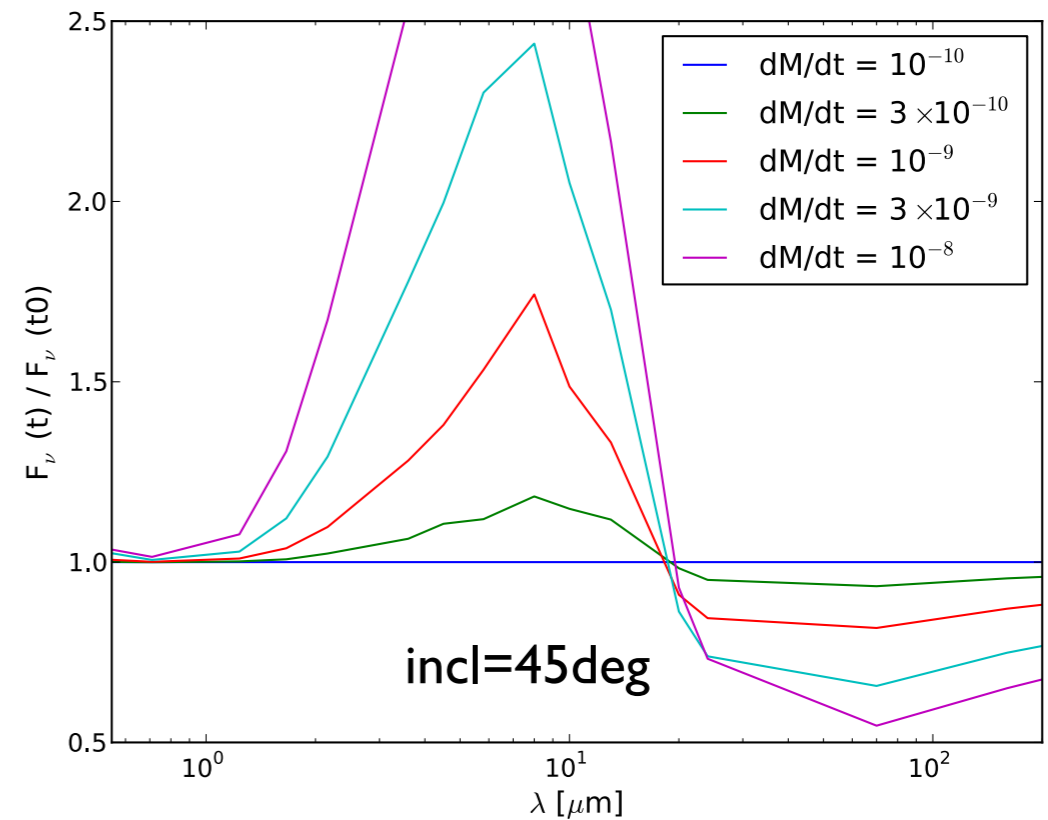
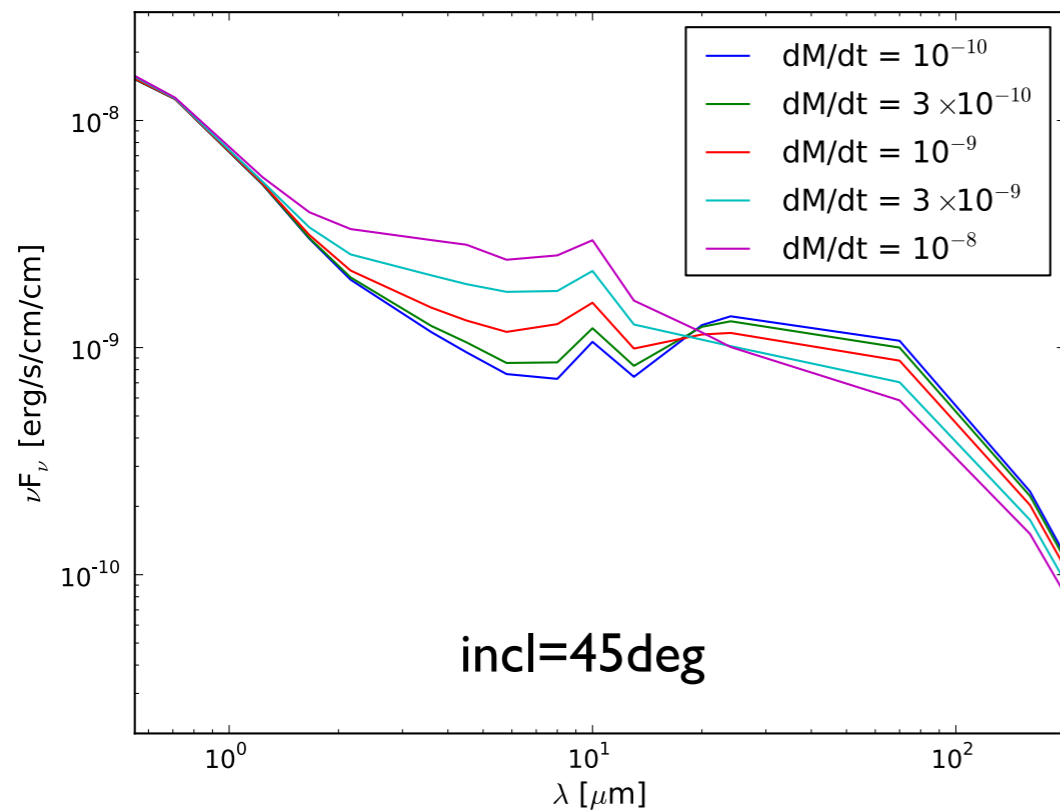
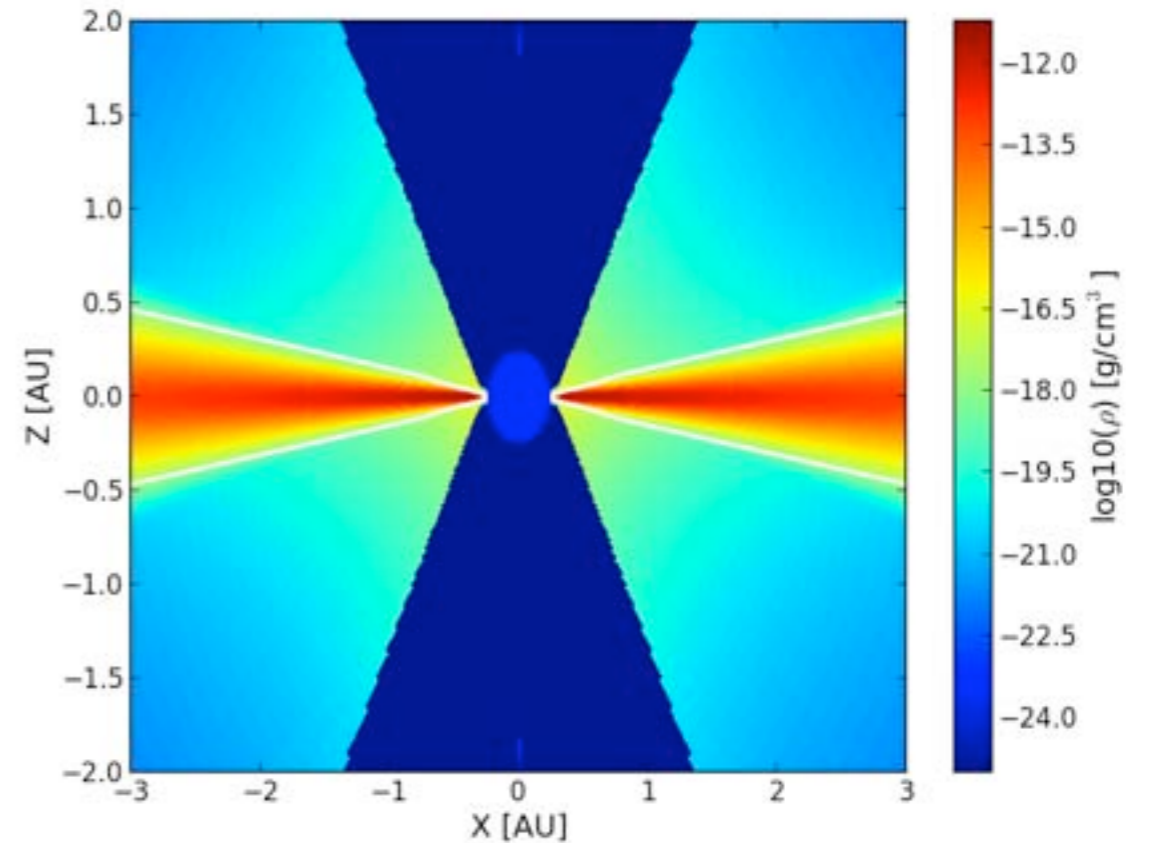
Disk wind

Model:

Kurosawa et al. 2006

Simple magnetocentrifugal wind

Varied the outflow-rate between $10^{-10} M_{\odot}/\text{yr}$ and $10^{-8} M_{\odot}/\text{yr}$



Variable inner rim

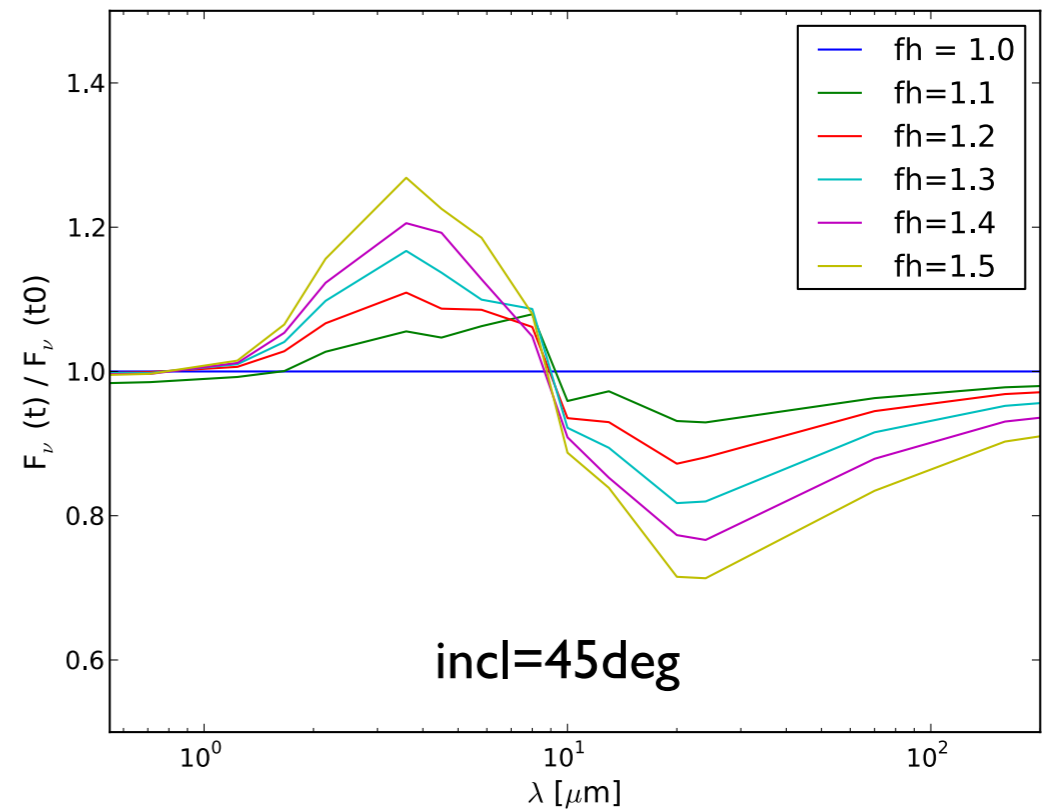
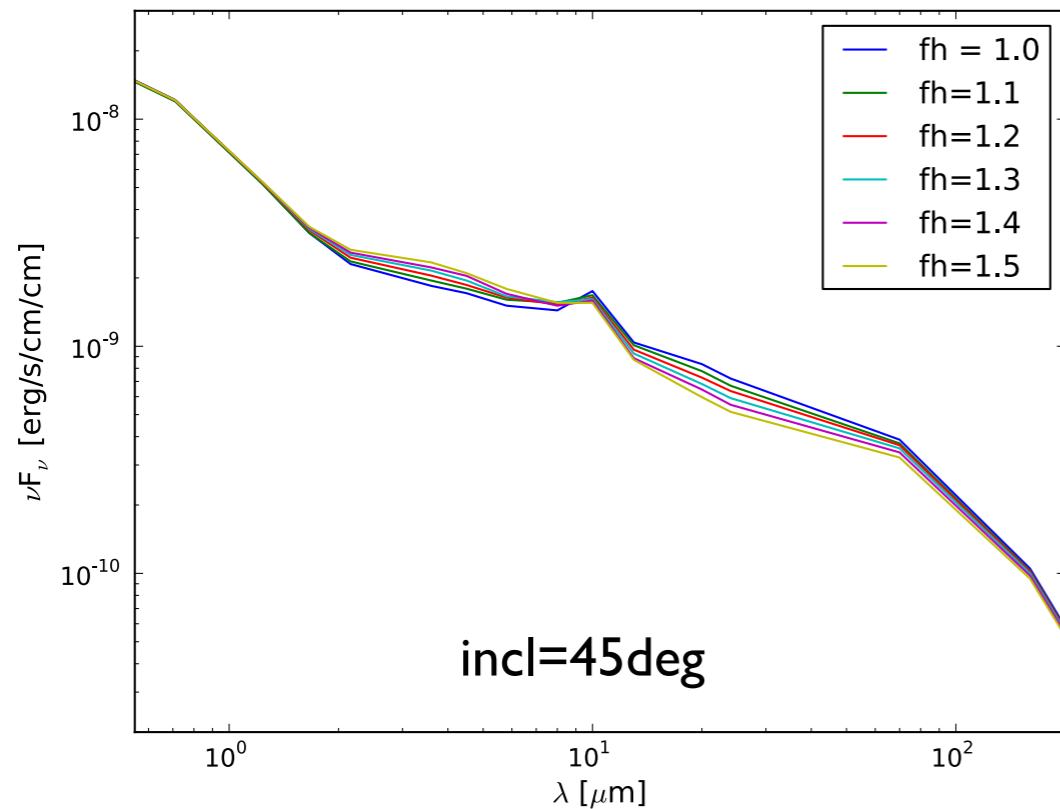
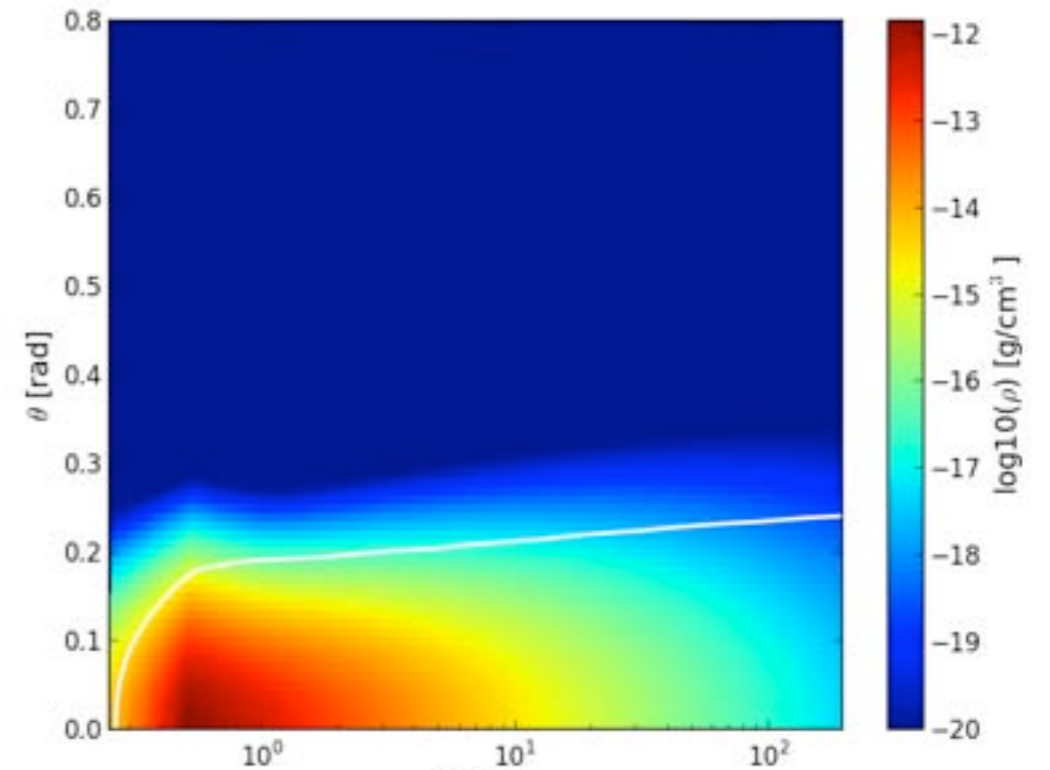
Model:

$$\rho(r, z, \phi) = \frac{\Sigma(r)}{H_p \sqrt{2\pi}} \exp\left[-\frac{z^2}{2H_p^2}\right]$$

$$\frac{H_p}{r} = \frac{H_{p,\text{out}}}{r_{\text{out}}} r^{1/7}$$

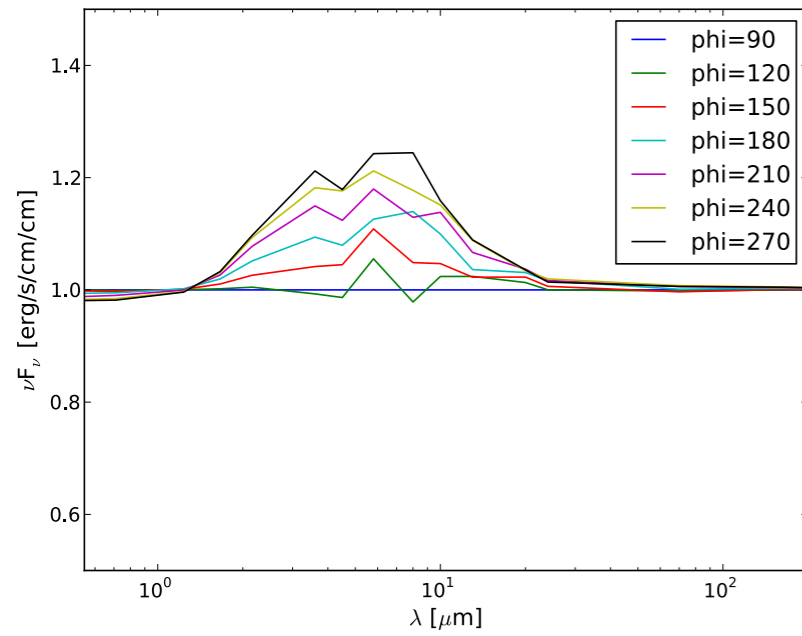
$$\frac{H_p}{r} = \frac{H_{p,\text{in}}}{r_{\text{in}}} r^\zeta$$

Increased $H_{p,\text{in}}$ up to 1.5 times the unperturbed value

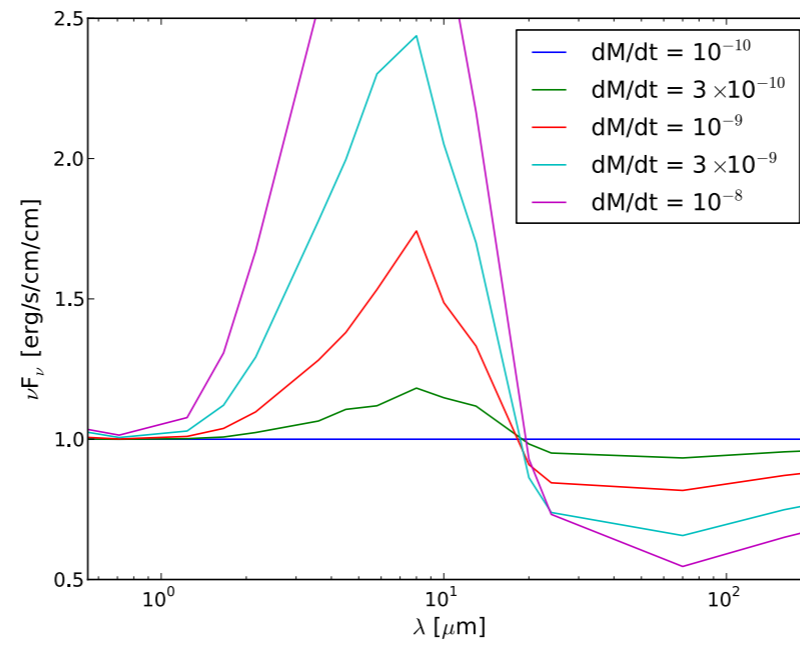


Photometric variability

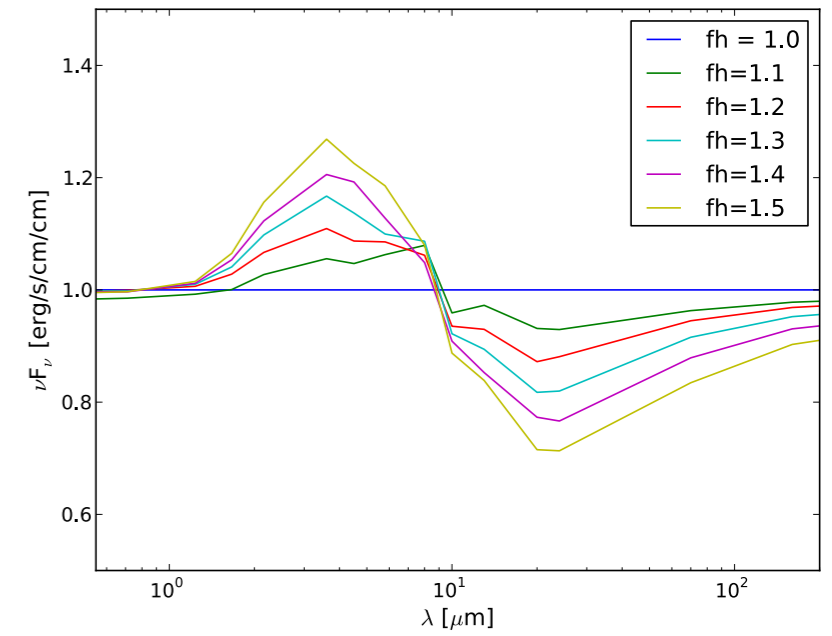
Warp



Wind



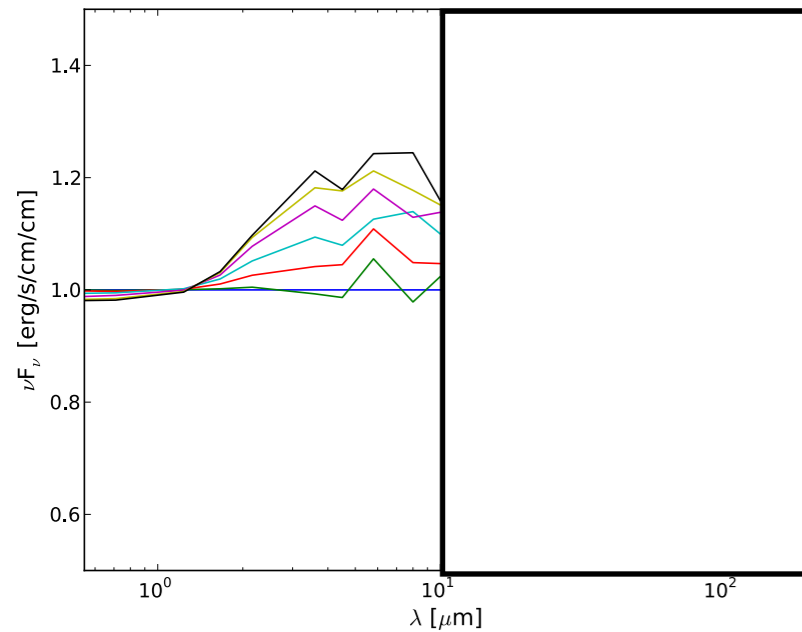
Variable rim



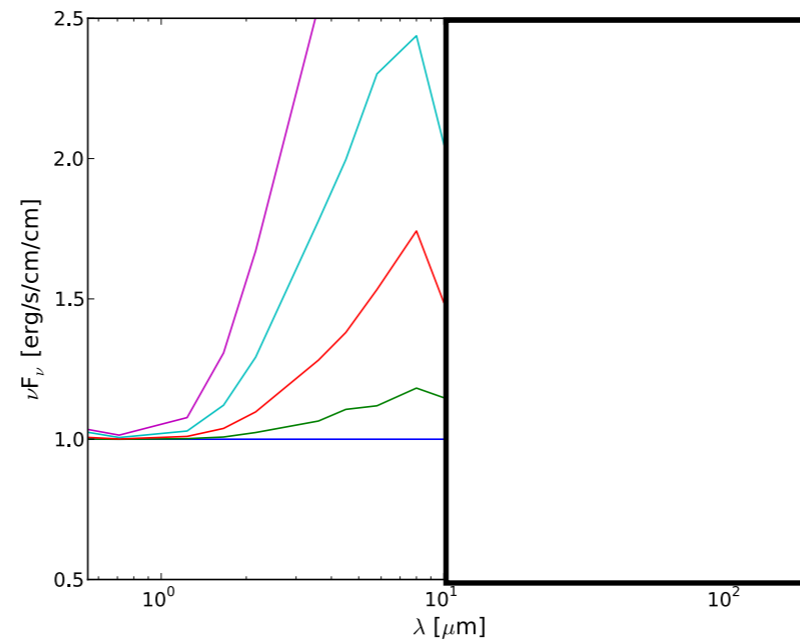
All models can provide a variability amplitude of 10-20%

Photometric variability - without Spitzer

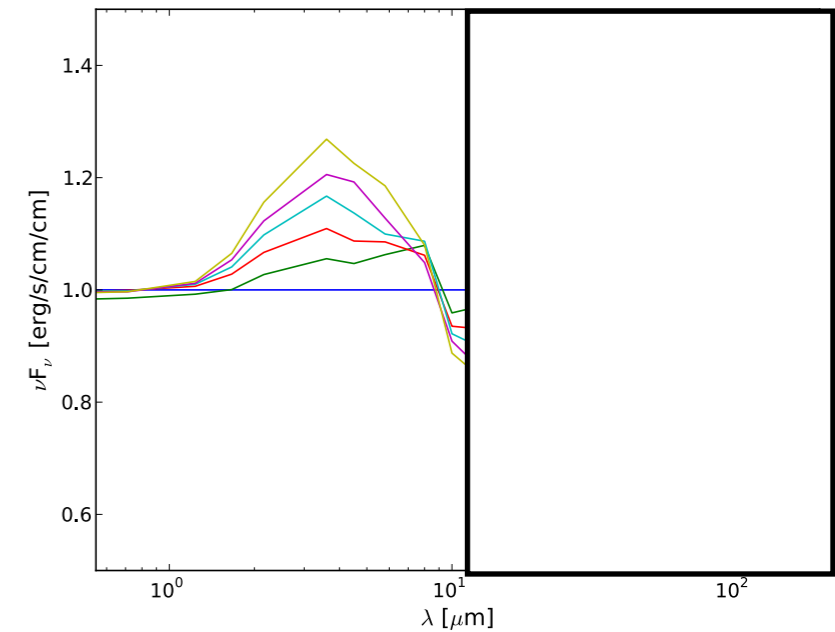
Warp



Wind



Variable rim



All models can provide a variability amplitude of 10-20%

Shortwards of $\sim 10 \mu\text{m}$ the wavelength dependence of the variability amplitude is similar for different models.

Interferometric variability

Method I (Fourier plane)

Measure the visibility amplitude and closure phase *at the same* uv-coordinates at different times and constrain the structure from the variation of these quantities

Advantage: only a few uv-points can be sufficient to distinguish between models

Disadvantage: Scheduling constraints

Method II (Image plane)

Reconstruct the image at each epoch of the observing campaign and try to detect the variable component in the images

Advantage: Easier scheduling than the Fourier method

Disadvantage: More uv points are required than for Method I
Issues with visibility averaging

Interferometric variability

Method I (Fourier plane)

Measure the visibility amplitude and closure phase *at the same* uv-coordinates at different times and constrain the structure from the variation of these quantities

Advantage: only a few uv-points can be sufficient to distinguish between models

Disadvantage: Scheduling constraints

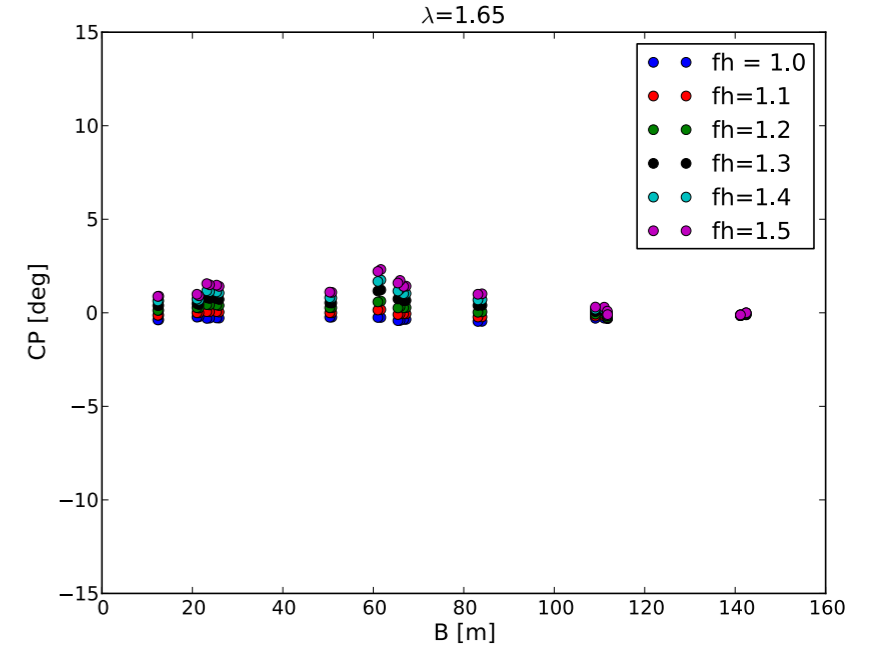
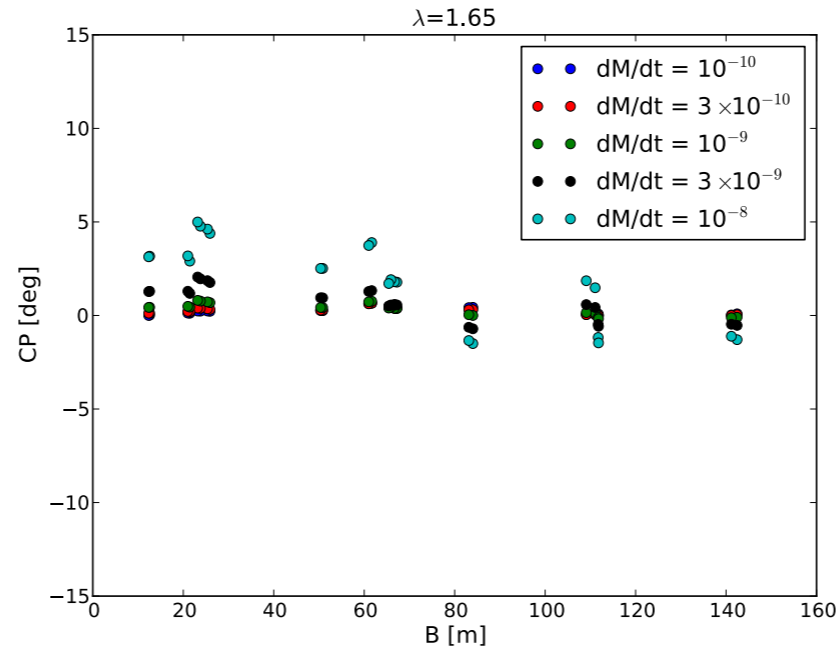
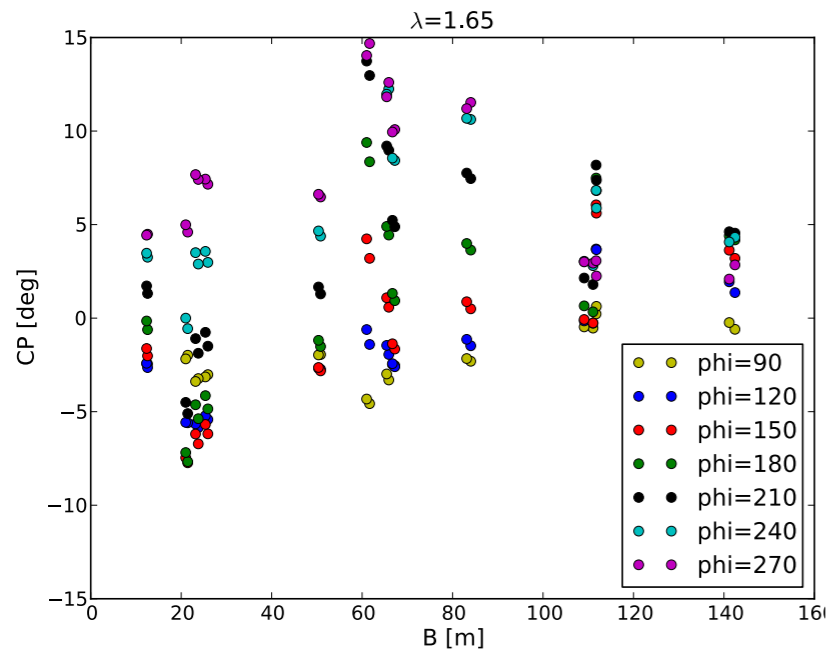
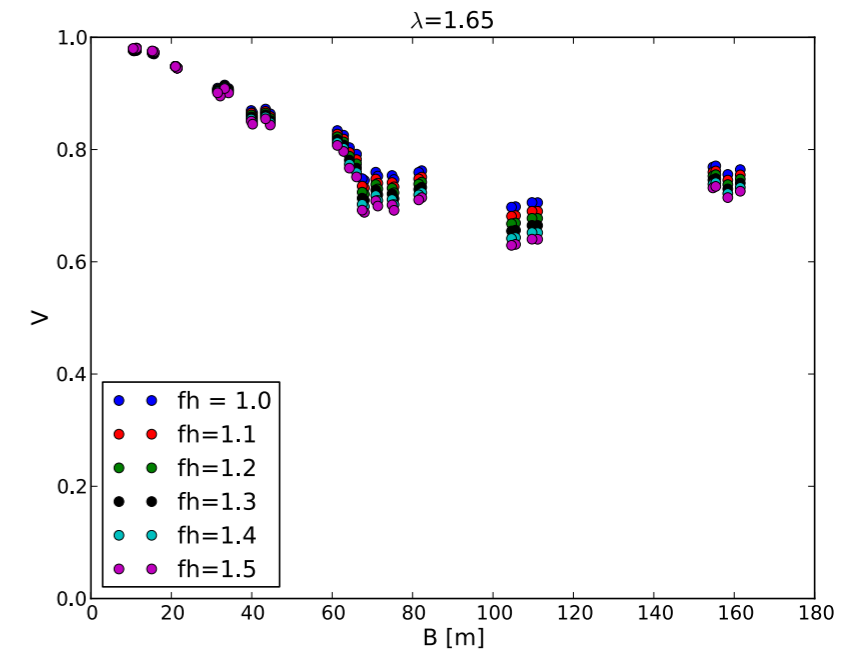
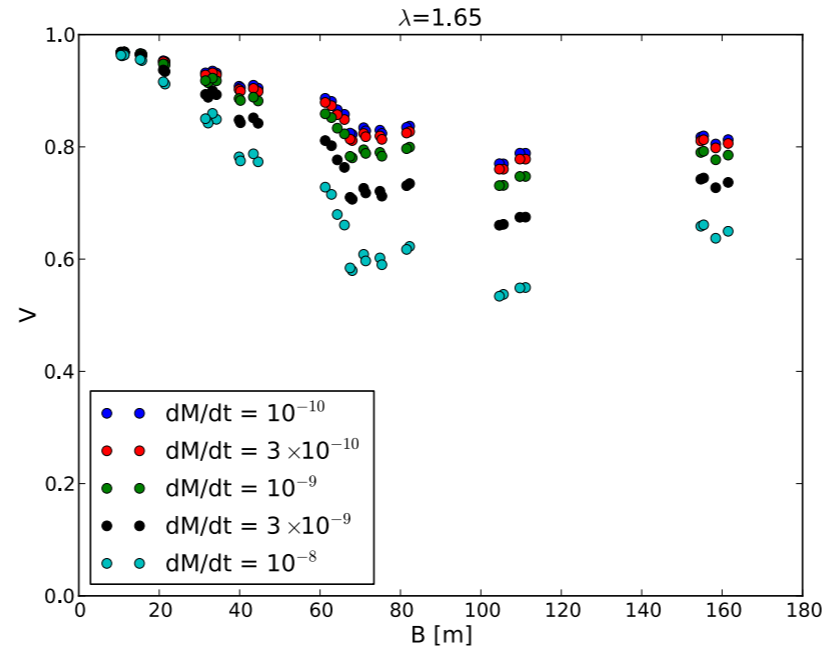
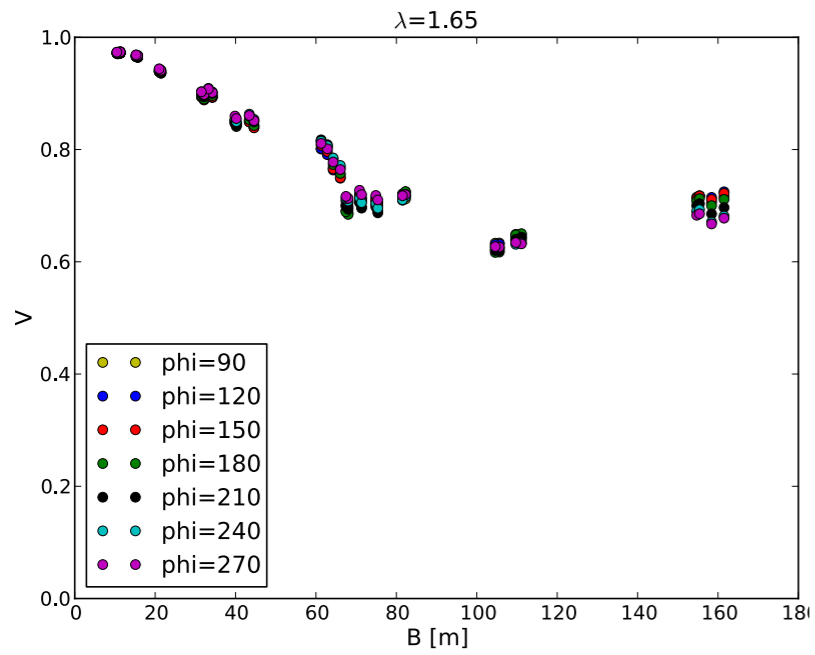
Chose three quadruplets (small, medium, large) and followed the source through half of the period to see how V and CP would change

Interferometric variability

Warp

Wind

Variable rim



Conclusions

All three studied perturbation can induce significant photometric variability.

The amplitude of the variability depends on the inclination for non-axisymmetric perturbations

The wavelength dependence of the variability amplitude can be similar for different models at NIR/MIR wavelengths

Multi-epoch NIR/MIR interferometry can be used to differentiate between models:

- Rotating azimuthal asymmetries generate strong variation in the CP with low level perturbation in the visibility amplitude
- Axisymmetric radial perturbation (e.g. disk wind) induce strong variation in the visibility amplitude with small CP perturbation.
- For high inclinations the variability signature of axisymmetric and non-axisymmetric perturbation in NIR interferometric observations becomes very similar to each other